Gravitational Stability of Suspensions of Attractive Colloidal Particles

Chanjoong Kim,[1,2] Yaqian Liu,[3] Angelika Kühnle,[3,*] Stephan Hess,[3] Sonja Viereck,[3] Thomas Danner,[3] L. Mahadevan,[2] and David A. Weitz[1,2]

[1]*Department of Physics, Harvard University, Cambridge, Massachusetts 02138, USA*
[2]*DEAS, Harvard University, Cambridge, Massachusetts 02138, USA*
[3]*BASF AG, 67056 Ludwigshafen, Germany*

(Received 15 February 2007; published 11 July 2007)

Colloidal suspensions are susceptible to gravitationally induced phase separation. This can be mitigated by the formation of a particle network caused by depletion attraction. The effectiveness of this network in supporting the buoyant weight of the suspension can be characterized by its compressional modulus. We measure the compressional modulus for emulsion networks induced by depletion attraction and present a model that quantitatively predicts their gravitational stability. We also determine the relationship between the strength of the depletion attraction and the magnitude of the compressional modulus.

DOI: 10.1103/PhysRevLett.99.028303 PACS numbers: 82.70.Dd, 47.56.+r, 82.70.Kj

Any colloidal suspension is susceptible to gravitationally induced sedimentation or creaming, which can lead to phase separation of the particles, even if they are otherwise stable against aggregation or coalescence. This is particularly important for commercial products, where gravitational stability can ultimately limit shelf life. Gravitational stability can be enhanced by density matching the particles to the suspending fluid, by restricting the particle size so that their Brownian motion helps keep them suspended, or by increasing the viscosity of the suspending fluid to slow phase separation. However, these methods are often not feasible. An alternate method that is frequently used is to cause a weak attraction between the particles, resulting in a solidlike network or gel of the particles themselves, which helps support their buoyant weight [1]. The network can still easily yield under shear, allowing the suspension to flow. A convenient means of inducing the requisite interparticle attraction is through the depletion interaction [2], caused by the addition of nonadsorbing particles or polymer to the suspension. Indeed, polymers added to the suspension to increase its viscosity to slow the phase separation may also induce a depletion attraction, leading to gelation, and thereby providing an alternate means of stabilization. The ability of the network to support its buoyant weight is characterized by its compressional modulus [1], from which we determine the stress the network can support as a function of the particle volume fraction, ϕ. The ϕ-dependence of the stress is analogous to the equation of state for equilibrium particles, where osmotic pressure balances buoyant stress [3], and this has been measured for hard spheres [4,5]. The compressional modulus has also been measured for networks of strongly attractive particles [1]. The gravitationally induced instability of weak depletion-attraction-induced networks has also been extensively investigated [6–8]. However, for these systems there has been no investigation of the compressional modulus, its relationship to depletion attraction, and its role in gravitational stability with changing ϕ. Understanding these effects is essential to fully exploit this means of stabilization.

In this Letter, we measure the volume-fraction dependence of the compressional modulus of a depletion-attraction-induced emulsion network and use this to determine the gravitational stability of the suspension. We calculate the time evolution of the height-dependent volume fraction of the suspension, and obtain excellent agreement with the data. We gain insight into the origin of the effect by determining the relationship between the depletion-attraction and the compressional modulus.

We use a colloidal suspension composed of a nearly monodisperse emulsion of paraffin oil in water at a volume fraction of $\phi_0 = 0.2$, stabilized with a commercial nonionic surfactant (Lutensol TO8). We use two different emulsion samples with hydrodynamic radii of $R = 360$ nm or $R = 170$ nm, and with polydispersities of $\sim 30\%$ of the mean, as measured with dynamic light scattering (DLS). The density mismatch of the oil is $\Delta\rho = 0.16$ g/cm^3. To induce a depletion interaction, we add either a nonabsorbing polymer or one of two different surfactants to a concentration c_m, above the critical micelle concentration (cmc ~ 0.08 mM). The depletant polymer is polyvinylpyrrolidon (PVP) with molecular weight of 10^6 g/mol and $r = 25$ nm as measured by DLS. The first surfactant (Lutensol TO8) has a micelle size of $r = 4.5$ nm, while the second (Lutensol A8) has $r = 6$ nm, as measured by DLS.

To determine the strength of the depletion attraction, we use static light scattering to measure the osmotic compressibility [9] of the polymer and micelles as functions of concentration, using literature values of dn/dc_m [10,11], where n is the index of refraction. We integrate this to obtain the osmotic pressure, Π_o, and calculate the maximum strength of the depletion interaction between oil drops, $U = \Pi_o V_{\text{dep}}$, where $V_{\text{dep}} = 2\pi R r^2$ [12].

To monitor the gravitational stability, we record images of the emulsions as they cream, and measure the position of the interface between the emulsion and the clear fluid subnatant. We use 23-mm diam cylindrical vials, and confirm that the size does not impact the results by varying the

diameter by a factor of 2. We also confirm that the curved meniscus does not affect the results by repeating the experiment using a sample filled to the top of a sealed vial. We vary the initial height, H_0, of the emulsion from 5 to 57 mm, and monitor the time evolution of the height, $H(t)$, measured from the top of emulsion as shown in the left inset of Fig. 1. When the depletion attraction is not too large, the taller samples initially cream slowly, and then exhibit delayed collapse [6], where the sample precipitously creams to a more compressed state, shown for samples with $R = 360$ nm and $r = 4.5$ nm (solid points Fig. 1). Less tall samples cream monotonically, reaching a new steady-state height, with no delayed collapse (open points Fig. 1).

Varying H_0 allows us to vary the buoyant stress in the emulsion. Since the sample is a gel, the emulsion at the top of the sample is subject to the full buoyant stress of all the suspensions below. As the sample creams, the volume fraction at the top must increase from its initial value, ϕ_0, to the final value, ϕ_∞, reflecting the local compressive strain. The ability of the sample to withstand this compression is determined quantitatively by the compressional modulus, $K(\phi) = -\phi\partial\sigma/\partial\phi$ [1]; this reflects the change of ϕ with applied stress, σ, and is similar to the bulk modulus of the network alone but for a uniaxial stress. We can determine $K(\phi_\infty)$ by measuring ϕ_∞ in the steady state at the top of the sample as a function of H_0, which sets the magnitude of the stress, $\sigma = \Delta\rho g\phi_0 H_0$. After the sample reaches steady state we measure ϕ_∞ by skimming a small amount of sample from the top within 2 mm, weighing it, drying it, and reweighing it. The magnitude of σ increases dramatically with ϕ_∞ for all samples, as shown in Fig. 2. The specific behavior depends on both r and c_m, but, in each case, the data appear to diverge as ϕ_∞ approaches $\phi_c \approx 0.64$, the maximum value for random close packing of uniform spheres. To account for this divergence, we fit the data with the functional form

$$\sigma(\phi_\infty) = -\alpha\frac{\phi_\infty - \phi_g}{\phi_c - \phi_\infty}, \tag{1}$$

where the stiffness parameter, α, is a constant that depends on r and c_m. We have included a minimum concentration required for gelation, $\phi_g = 0.03$, which we determine empirically from the initial creaming behavior and find to be independent of r and c_m in our experimental range; samples with $\phi_0 \leq \phi_g$ cream much more rapidly, presumably because the attraction induces clusters that do not gel but instead rapidly cream. We obtain excellent agreement with the data as shown in Fig. 2. To highlight the divergence as ϕ_∞ approaches ϕ_c, we scale each data set by its value of α, and plot the results as a function of $\phi_c - \phi_\infty$ on a logarithmic plot. The data all overlay on a single master curve, exhibiting nearly linear behavior, as shown in the inset in Fig. 2. The solid line through the data is a fit using the form in Eq. (1). This functional form allows us to determine the compressional modulus directly,

$$K(\phi_\infty) = \alpha\phi_\infty\frac{(\phi_c - \phi_g)}{(\phi_c - \phi_\infty)^2}. \tag{2}$$

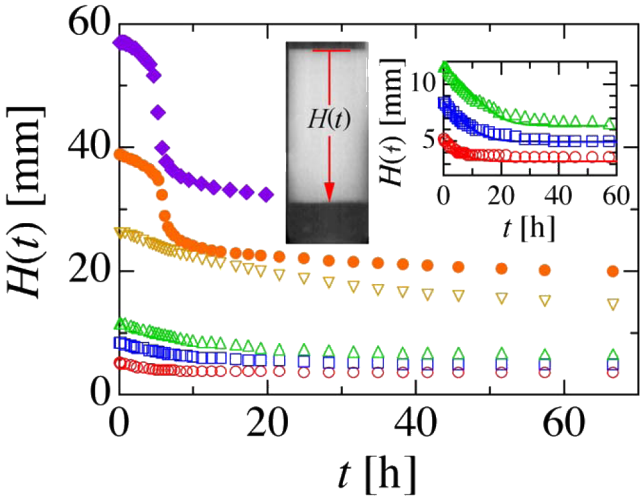

FIG. 1 (color online). Time evolution of the heights of an emulsion gel with various initial height H_0 but the same composition, $\phi_0 = 0.2$, $c_m = 0.06$ g/ml, $r = 4.5$ nm, and $R = 360$ nm. H_0 are 5, 9, 12, 26, 39 and 57 mm from bottom to top, respectively. Left inset: Picture of a sample. Right inset: Measured $H(t)$ compared with the values calculated with the nonlinear poroelastic model for the samples that do not exhibit a delayed collapse.

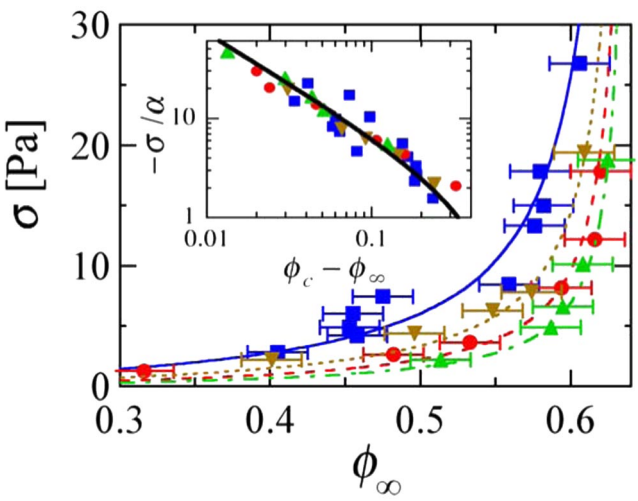

FIG. 2 (color online). Gravitational stress as a function of ϕ_∞ in the steady state at the top of emulsion gels with: $r = 4.5$ nm and $c_m = 0.016$ g/ml (■), $r = 6$ nm and $c_m = 0.016$ g/ml (▼), $r = 4.5$ nm and $c_m = 0.06$ g/ml (●), $r = 6$ nm and $c_m = 0.06$ g/ml (▲). For all samples, $R = 360$ nm. Lines are fits to Eq. (1) with $\alpha = 1.8$, 1, 0.6, and 0.4 Pa for ■, ▼, ●, and ▲, respectively. Inset: Log-log plot of gravitational stress normalized with α as a function of $\phi_c - \phi_\infty$, where $\phi_c = 0.64$.

Knowledge of $K(\phi_\infty)$ also allows us to predict the full height dependence of ϕ_∞. We balance the differential stress with the buoyant weight across a length dz,

$$d\sigma = -\frac{K(\phi_\infty)}{\phi_\infty} d\phi_\infty = \Delta\rho g \phi_\infty dz. \tag{3}$$

We integrate Eq. (3) by separation of variables, using Eq. (2) for $K(\phi_\infty)$, yielding

$$\frac{\phi_c(\phi_\infty - \phi_0)}{(\phi_c - \phi_\infty)(\phi_c - \phi_0)} + \ln\frac{\phi_\infty(\phi_c - \phi_0)}{\phi_0(\phi_c - \phi_\infty)} = \frac{\Delta\rho g(z-H)\phi_c^2}{\alpha(\phi_c - \phi_g)}, \tag{4}$$

where H is the final height of the sample. This allows us to calculate the full profile of the height dependence of ϕ_∞, using the values of α obtained from the fits in Fig. 2. To test this prediction, we compare the results with experimental measurements, which are obtained by extracting small volumes of the sample at different heights using a long syringe, and determining their ϕ_∞. The agreement is excellent, as shown by the comparison between the data points and the lines in Fig. 3 for samples with $R =$ 360 nm, $c_m = 0.16$ g/ml and for $r = 4.5$ and 6 nm. We obtain equally good agreement with this functional form for all other emulsions, where we vary R, c_m, and r, and use only the single fitting parameter, α. We also obtain excellent agreement between the measured and calculated values of H and ϕ at the top of the sample, as shown in the inset to Fig. 3.

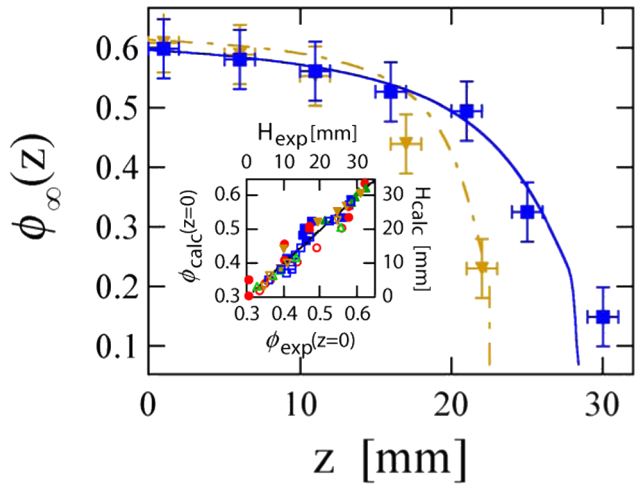

FIG. 3 (color online). Height profiles of ϕ_∞ for emulsion with $R = 360$ nm, $r = 4.5$ nm, $c_m = 0.16$, and $H_0 = 70$ mm (■), and $R = 360$ nm, $r = 6$ nm, $c_m = 0.16$, and $H_0 = 57$ mm (▼). The lines are fits to Eq. (4). Inset: Comparison between calculations and measurements of final volume fractions (filled symbols) at the top of emulsion gels and final heights (empty symbols). Symbols are the same as in Fig. 2. The dashed line corresponds to the exact match between calculation and measurement.

We can also use the compressional modulus to determine the evolution of the height of the sample as it begins to cream. Provided there is no sudden collapse, this evolution is described by the theory for poroelasticity [13], which accounts for the relative flow of fluid through the network. However, since the relative change of the volume fraction, ϕ, is large, we extend the theory to account for changes in ϕ. The stress across any region of the sample, $\partial\sigma/\partial z$, reflects a balance of the gravitational stress with the pressure, p, due to fluid flow through the network, and the elastic stress of the gel due to depletion,

$$-\Delta\rho g\phi = \frac{\partial p}{\partial z} + \frac{K(\phi)}{\phi}\frac{\partial\phi(z)}{\partial z}. \tag{5}$$

We note that Eq. (3) is a steady-state case of Eq. (5), at which there is no fluid flow and the pressure gradient is zero. The pressure due to the fluid flow is given by Darcy's law, which relates the fluid velocity to the pressure gradient [13]. However, since ϕ is changing, we must also ensure continuity, giving

$$\frac{\partial\phi}{\partial t} + \frac{\partial}{\partial z}\left(\frac{\phi\kappa(\phi)}{\eta}\frac{\partial p}{\partial z}\right) = 0, \tag{6}$$

where $\kappa(\phi)$ is the permeability of the network, and η is the fluid viscosity. Combining Eqs. (5) and (6) results in a diffusion advection equation for p,

$$\frac{\partial p}{\partial t} - \frac{K(\phi)}{\phi}\frac{\partial}{\partial z}\left(\frac{\phi\kappa(\phi)}{\eta}\frac{\partial p}{\partial z}\right) - \frac{\Delta\rho g\phi\kappa(\phi)}{\eta}\frac{\partial p}{\partial z} = 0. \tag{7}$$

Here the second term is a diffusive contribution, reflecting the effect of the compressional modulus to evenly spread the suspension, while the third term is the advective contribution, reflecting the tendency to cream due to the gravitational stress. To solve Eq. (7), we use a constant initial pressure gradient $\partial p/\partial z|_{t=0} = \Delta\rho g\phi_0$ throughout the sample and take $\partial p/\partial z|_{z=0} = 0$ at the top of the sample, while $p_{z=H} = 0$ remains constant at the bottom of the emulsion. We approximate the permeability as $\kappa(\phi) = \kappa_0(\phi_0/\phi)^{2/(3-d_f)}$ [13], where d_f is the network fractal dimension. From the initial velocity of the creaming profiles, we estimate $\kappa_0 = 5 \times 10^{-13}$ m^2 [13] and from analysis of images of the network using either box counting or the structure factor, obtained by Fourier transforming the image [14], we estimate $d_f \approx 1.8$. We solve Eqs. (6) and (7) numerically, calculate the height of the sample from conservation of material, $\int_0^{H(t)} \phi dz = \phi_0 H_0$, and obtain excellent agreement with the measured data, as shown by the solid lines in the right inset in Fig. 1, provided there is no delayed collapse, which is not described within this picture.

The behavior of these gels is characterized by their compressional modulus, which determines the stress they can support, $\sigma(\phi)$. There is a direct analogy with equilib-

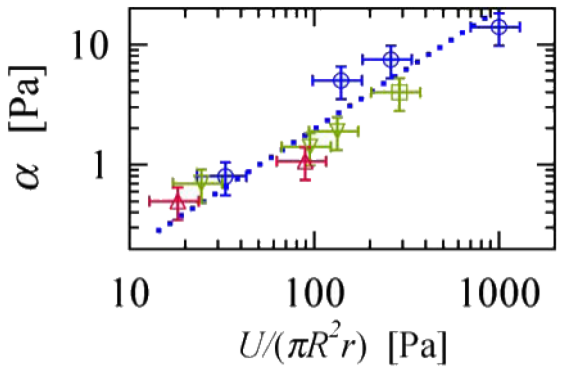

FIG. 4 (color online). Scaling of the stiffness parameter, α, predicted by Eq. (8). The samples with TO8 micelles ($\bigtriangledown$) have $R = 360$ nm and $r = 4.5$ nm with $c_m = 0.06$, 0.13, and 0.16 g/ml from a lower value to higher one. Those with A8 micelles ($\bigtriangleup$) have $R = 360$ nm and $r = 6$ nm with $c_m = 0.06$ and 0.16 g/ml. The sample with small particles ($\square$) has $R = 170$ nm and $r = 4.5$ nm with $c_m = 0.16$ g/ml. The final sample with PVP ($\bigcirc$) has $R = 360$ nm and $r = 25$ nm with $c_m = 0.016$, 0.03, 0.04, and 0.08 g/ml.

rium hard-sphere colloidal particles, where the equation of state determines the ϕ dependence of their osmotic pressure, $\Pi(\phi)$ [4,5]. This can be determined from the height dependence of ϕ [4]. By contrast, particle gels are not in equilibrium, so their height dependence can not determine an equation of state; instead it reflects the steady-state behavior of the network. For the network, $\sigma(\phi)$ is analogous $\Pi(\phi)$, but again is not an equilibrium quantity. Interestingly, however, both $\sigma(\phi)$ and $\Pi(\phi)$ exhibit the same divergence with volume fraction, $(\phi_c - \phi)^{-1}$ [15]. For hard spheres, this divergence reflects the consequences of the repulsive interaction between particles, as they are increasingly crowded together [16]. It presumably reflects the same effects for the networks; even though there is an attractive interaction between particles, when ϕ becomes increasingly large, the repulsive interaction dominates. Finally, the emulsion droplets are themselves deformable; however, their deformability scales as the Laplace pressure, γ/R, where γ is the surface tension. Since $\gamma/R \sim 10^4$ Pa while σ is typically no larger than 100 Pa, drop deformation is unlikely to play a role in the behavior.

Despite the apparent similarity with repulsive hard spheres, the attractive interaction does, nevertheless, play a critical role in the behavior. In the case of hard-sphere suspensions, both $\Pi(\phi)$ and $K(\phi)$ scale as the thermal energy, k_BT/R^3. By contrast for the emulsion gels, $\sigma(\phi)$ and $K(\phi)$ scale with the stiffness parameter, α. This constant should reflect the attractive interaction between neighboring particles. Since it has units of stress, we expect it to scale as the force between two neighboring particles divided by the area of the interparticle bond. From dimensional analysis, the force scales with the bond energy divided by the width of the bond, U/r, while the area scales with R^2, and

$$\alpha \sim U/rR^2. \tag{8}$$

We obtain excellent agreement with this prediction for all experimental samples, using both micelles and polymer as depletants, as shown in Fig. 4. Physically, this behavior implies that the compressional modulus reflects two effects: Squeezing the particles together must require local rearrangements in particle positions, which is counteracted by the attractive interaction, reflected through the contribution of α. In addition, the particles are themselves squeezed together, which is counteracted by the local repulsive interaction, reflected by the $(\phi_c - \phi)^{-2}$ scaling. The agreement between the data using polymer and micelles as depletants confirms the generality of this behavior.

The results presented here provide a means to quantitatively predict stability of depletion-attraction colloidal gels against gravitationally induced phase separation. They highlight the role of the attractive interaction between particles. However, they do not address the important issue of delayed collapse, which can also impact stability.

Partial support for this work came from the Harvard MRSEC (No. DMR-021385) and the NSF (No. DMR-0602684).

*Present address: Department of Physics, University of Osnabrück, 49076 Osnabrück, Germany.

[1] R. Buscall, Colloids Surf. **5**, 269 (1982).
[2] V. Prasad *et al.*, Faraday Discuss. **123**, 1 (2003).
[3] W. B. Russel *et al.*, *Colloidal Dispersions* (Cambridge University Press, Cambridge, New York, 1989).
[4] M. A. Rutgers *et al.*, Phys. Rev. B **53**, 5043 (1996).
[5] R. Piazza *et al.*, Phys. Rev. Lett. **71**, 4267 (1993).
[6] W. C. K. Poon *et al.*, Faraday Discuss. **112**, 143 (1999).
[7] L. Starrs *et al.*, J. Phys. Condens. Matter **14**, 2485 (2002).
[8] N. A. M. Verhaegh *et al.*, Physica (Amsterdam) **264A**, 64 (1999).
[9] W. Brown, *Light Scattering: Principles and Development* (Oxford University, New York, 1996).
[10] R. R. Balmbra *et al.*, Trans. Faraday Soc. **60**, 979 (1964).
[11] W. H. Richtering *et al.*, J. Phys. Chem. **92**, 6032 (1988).
[12] P. Walstra, in *Encyclopedia of Emulsion Technology*, edited by P. Becher (Marcel Dekker, New York, 1996), Vol. 4.
[13] S. Manley *et al.*, Phys. Rev. Lett. **94**, 218302 (2005).
[14] D. ben-Avraham and S. Havlin, *Diffusion and Reactions in Fractals and Disordered Systems* (Cambridge University Press, Cambridge, England, 2000).
[15] L. V. Woodcock, Ann. N.Y. Acad. Sci. **371**, 274 (1981).
[16] K. E. Davis and W. B. Russel, Phys. Fluids A **1**, 82 (1989).